PHYSICAL REVIEW A VOLUME 42, NUMBER 11 1 DECEMBER 1990

Classical and quantum-mechanical dynamics of a quasiclassical state of the hydrogen atom

Z. Dačić Gaeta and C. R. Stroud Jr.
The Institute of Optics, University of Rochester, Rochester, New York 14627
(Received 14 June 1990)

We explore the classical limit of the hydrogen atom by constructing a minimum-uncertainty wave packet that travels along a Kepler orbit. The dynamics of the wave packet display both classical and quantum-mechanical properties. Over a limited period of time, during which the dynamics of the wave packet may be considered linear, the motion of the wave packet can be described by classical equations of motion. After this time, the quantum dynamics, whose most prominent features are decays and revivals of the wave packet, becomes dominant. We discuss decays and revivals of the wave packet in detail.

I. INTRODUCTION

Bohr formulated the correspondence principle[1] with the intention of tying together the old quantum theory of matter with classical electrodynamics. By virtue of the correspondence principle, the properties of the motion of the electron were related to the properties of the emitted radiation, which made possible accurate calculations of intensities of spectral lines.[2] Although its original significance was diminished by the development of quantum mechanics, the main point of the correspondence principle, that classical mechanics is the large-quantum-number limit of quantum mechanics, is still one of the fundamental concepts in quantum theory.

Recent advances in experimental techniques, in particular the development of tunable and short-pulse lasers, have given physicists the opportunity to perform experiments on single atoms and to study interactions between highly excited atoms and radiation. As a result of this development, the correspondence principle, together with other fundamental concepts of quantum theory, has become subject to experimental verification.

Results of research on chaos pose a challenge to the correspondence principle. There is a general consensus among theorists that chaos does not exist in quantum systems in the same sense that it does in classical ones. Modeling of experimental results with classical calculations has been performed with mixed success; the microwave ionization of highly excited hydrogen is an example of both excellent (the low-frequency limit[3]) and poor (the high-frequency limit[4]) agreement. The apparent discrepancy in the behavior of a chaotic classical system and its large-quantum-number counterpart make the study of the classical limit of quantum mechanics an urgent task.

The first step in exploring the quantum-classical border is to construct a wave packet that behaves like a classical system, in the sense that the outcome of a single measurement of the position or momentum of the wave packet can be accurately predicted by the classical equations of motion. In order to specify the state that describes this wave packet more formally, we will demand that it satisfy the following properties. First, it should be a well-localized wave packet in the configuration space. Second, it should be a minimum-uncertainty wave packet in the phase space. This is the best possible approximation of a point in the coarse-grained quantum phase space of cell size $\hbar/2$. Third, the quasiclassical state should be dynamically similar to the corresponding classical system, namely, it should move along the corresponding classical orbit. We will refer to a quantum state with the above properties as a quasiclassical state.

A coherent state of the linear harmonic oscillator possesses the specified properties. A coherent state of the linear harmonic oscillator is a minimum-uncertainty wave packet whose center of mass travels along the trajectory of the corresponding classical oscillator. As the expectation value of the number operator increases, the uncertainties in the measurement of the position and momentum remain constant and thus become relatively smaller with respect to the expectation value of the amplitude of oscillation, and eventually become insignificant for a truly macroscopic system. Coherent states of the linear harmonic oscillator have another important classical property: the shape of the wave packet is invariant, due to the fact that the separation between energy levels is constant as a consequence of linearity of the Hamiltonian in action-angle variables.

A linear-harmonic-oscillator coherent state is an excellent example of how well the correspondence principle describes the macroscopic limit of a quantum-mechanical system, on account of which we might expect to find states with similar properties for other physical systems. This proves to be a difficult task for nonlinear systems.

In order to be localized in the configuration space, the wave-packet state must be a superposition of eigenstates, such that quantum numbers in all degrees of freedom must be large. For an arbitrary potential, the energies of the states that constitute the wave packet will not be equally separated, which implies that the shape of the packet will not be invariant during the evolution prescribed by the Schrödinger equation, and the uncertainty product will become greater than its minimum possible value. Thus, permanent localization is one property of a classical particle that we must yield in the search of a quasiclassical state of a quantum system.

However, if the time during which the spreading occurs increases with the quantum numbers of the states constituting the wave packet, then, in the limit of large quantum numbers, the wave packet is well defined over a long time.

II. QUASICLASSICAL STATE OF THE HYDROGEN ATOM

In the present paper we discuss only quasiclassical states for the three-dimensional Coulomb problem, although there are interesting results among the treatments of the radial Coulomb problem.[5]

In the paper in which he introduced coherent states of the linear harmonic oscillator, Schrödinger[6] suggested that a state with similar properties could be constructed for the hydrogen atom, and that this wave packet would travel along a Kepler elliptic orbit. In the same year, he mentioned in a letter to Lorentz[7] that in attempting to create such a wave packet he had encountered "great computational difficulties."

One of the first modern-day attempts to construct a quasiclassical state of the hydrogen atom was made by Brown.[8] This state consists entirely of circular-orbit eigenstates, i.e., standard hydrogenic eigenstates such that $l=m=n-1$, superimposed with a Gaussian weighting function. Brown's states are initially minimum-uncertainty wave packets that move along a circular Kepler orbit. The size of the orbit and the period of rotation correspond to the motion of a "classical" electron located at the center of mass of the wave packet.

General theories of coherent states were developed by Barut,[9] Perelomov,[10] and Nieto.[11] Barut's coherent states are constructed as eigenstates of the lowering operator. Coherent states of Perelomov are formed by acting on the ground state with the displacement operator. Nieto's procedure for constructing coherent states consists of finding minimum-uncertainty wave packets.

Mostowski[12] and McAnally and Bracken[13] construct their coherent states in the so(4,2) algebra, following the Perelomov and Barut general procedures, respectively. Neither of these states are minimum-uncertainty wave packets because the uncertainty product becomes infinitely large as $\langle N \rangle$, the expectation value of the principal action operator Γ_0, tends to infinity, although in Ref. 13 the ratio of the uncertainty and the corresponding expectation value tends to zero.

Gerry[14] and Bhaumik *et al.*[15] utilize the Kustaanheimo-Stiefel transformation[16] to map the three-dimensional Coulomb system into a four-dimensional linear harmonic oscillator with a constraint condition, and form a coherent state in the basis of this oscillator. The coherent state constructed this way is well localized. When the coherent state in Ref. 15 is constrained to lie in the xy plane, the expectation values of x and y have harmonic time dependence and satisfy the equation of a Kepler ellipse. Nandi and Shastry[17] show that this coherent state has minimum uncertainty in radius only if it is constrained to lie in the xy plane, and in this case only is the ellipse of motion the corresponding Kepler ellipse. The harmonic dependence of $\langle x \rangle$ and $\langle y \rangle$ pertains to the case of classical motion in a circle, whereas the condition that the orbit be in the xy plane is equivalent to the requirement that the angular momentum be parallel to the z axis. Thus, from a very general theoretical argument a result emerges that is in essence equivalent to the simple intuitive idea of Brown,[8] that the quasiclassical state of the hydrogen atom is a superposition of circular-orbit states.

Nauenberg[18] constructs coherent states in the o(3) algebra with M_x, M_y, and L_z as generators, where M_x and M_y are the x and y components of the Runge-Lenz vector. A coherent state of this type is a linear superposition of aligned hydrogenic eigenstates with large angular momentum in an n manifold. The probability distribution of this coherent state is well localized in radius and azimuthal angles, but suffers from poor localization in polar angle. Since the o(3) coherent states consists of eigenstates from the same n manifold, its shape is invariant in time. Nauenberg's coherent states are similar to the angularly localized wave packet of Yeazell and Stroud,[19] which was the first experimentally observed atomic wave packet. A wave packet localized in all three degrees of freedom is formed as a superposition of o(3) coherent states using a Gaussian weighting function. The motion of this wave packet is confined to a Kepler ellipse and the velocity of the center of mass varies along the orbit in the same way that the velocity of the corresponding classical particle does.

We indicated earlier that the shape of the quasiclassical hydrogen wave packet evolves in time as a result of the fact that the separation between energy levels is not constant. The wave function of the quasiclassical state is a quasiperiodic function of time. As a consequence of quasiperiodicity, the wave packet spreads and reassembles, thus displaying both classical and quantum features. All the wave packets we mentioned exhibit decays and revivals of coherence, which we study in detail in Sec. IV.

From the survey of the recent literature on the quasiclassical states of the hydrogen atom, we conclude that the "great computational difficulties" of Schrödinger can be overcome in the sense that a minimum-uncertainty wave packet can be formed that acts like a classical particle for a limited period of time. However, the generic nonlinearity of a physical system restricts the extent to which a quantum-mechanical system exhibits classical features, even in the limit of large quantum numbers.

We also see that three different approaches in Refs. 8, 15, and 18 all lead to wave packets that consist of aligned eigenstates with large angular momentum. The simplest of quasiclassical hydrogen states is Brown's circular-orbit wave packet. This state seems close to our earlier description of a classical limit of a quantum system. In the next two sections we study the localization and dynamics of Brown's quasiclassical states in detail, with special emphasis on fractional revivals of coherence.

III. LOCALIZATION OF BROWN'S QUASICLASSICAL STATE

Brown's quasiclassical state consists of circular-orbit eigenfunctions superimposed with a Gaussian weighting

function, which is centered at a large principal quantum number $\bar{n}$. The wave function that describes the wave packet is

$$|\Psi(t)\rangle=\frac{1}{(2\pi\sigma_n^2)^{1/4}}\sum_{n=1}^{\infty}\exp\left[-\frac{(n-\bar{n})^2}{4\sigma_n^2}\right]\times|\Psi_{n,n-1,n-1}e^{it/2n^2}, \quad (1)$$

where $\bar{n}$ and σ_n^2 are the mean and the standard deviation of the Gaussian distribution, respectively, and

$$\langle \mathbf{r}|\Psi_{n,n-1,n-1}\rangle=\Psi_{n,n-1,n-1}(r,\theta,\phi)=c_n r^{n-1}e^{-r/n}\sin^{n-1}\theta\, e^{i(n-1)\phi} \quad (2)$$

is an aligned standard hydrogenic eigenfunction ($l=m=n-1$) where c_n is a normalization constant.

A circular-orbit wave packet has uncertainty products that are almost minimal in all three degrees of freedom. We will show that the uncertainty product is a function of $\bar{n}$ and tends toward $\frac{1}{2}$ (in atomic units) as $\bar{n}$ tends to infinity.

First, we calculate the uncertainty in r and θ in a single circular-orbit state. Circular-orbit states are well localized in these two variables. When the well-known results[20] for the expectation values of r and r^2 for a standard hydrogenic eigenstate are used, one calculates the uncertainty in radius as $(\Delta r)_n=n/2\sqrt{2n+1}$. The expectation value of momentum $\langle \mathbf{p}\rangle$ is equal to zero in any standard hydrogenic eigenstate. The second-order moment of the radial momentum may be calculated as follows. The square of the radial momentum is equal to (atomic units are used throughout the paper)

$$p_r^2=\frac{2}{r}-2H-\frac{L^2}{r^2}$$

and its expectation value is equal to

$$\langle p_r^2\rangle_n=2\left\langle\frac{1}{r}\right\rangle_n-2\langle H\rangle_n-\langle L^2\rangle_n\left\langle\frac{1}{r^2}\right\rangle_n \quad (3)$$

since $[L^2,r]=0$. The uncertainty product in the radial degree of freedom is then equal to

$$(\Delta r\Delta p_r)_n=\frac{1}{2}\left[1+\frac{1}{2n}\right]+O\left[\frac{1}{n^2}\right],$$

where we have used the well-known results[20] for $\langle r^{-1}\rangle$ and $\langle r^{-2}\rangle$.

As circular-orbit states are superimposed in a wave packet with a Gaussian weighting function, this product will increase, although not significantly. The uncertainty in r can be calculated approximately by replacing the sum over n with an integral, and noting that off-diagonal matrix elements of r and θ are equal to zero in the $\{H,L^2,L_z\}$ basis. The uncertainty in radius, accurate to the first order in $1/\bar{n}$, is

$$\Delta r=[(\Delta r)_{\bar{n}}^2+4\bar{n}^2\sigma_n^2]^{1/2},$$

where σ_n is the standard deviation of the Gaussian distribution in Eq. (1). The uncertainty in radial momentum can be calculated to the same degree of accuracy as the uncertainty in radius by expanding $\langle p_r^2\rangle_n$ in a Taylor series in the neighborhood of $\bar{n}$ and replacing the sum by an integral. The uncertainty in radial momentum is found to be

$$\Delta p_r=\left[\frac{1}{2\bar{n}^2}\left[1+\frac{2}{\bar{n}}\right]+O\left[\frac{1}{\bar{n}^5}\right]\right]^{1/2}.$$

The uncertainty product in the radial degree of freedom is equal to

$$\Delta r\Delta p_r=\frac{1}{2}\left[1+\frac{1}{2\bar{n}}+\frac{4\sigma_n^2}{\bar{n}}\right]+O\left[\frac{1}{\bar{n}^2}\right]. \quad (4)$$

The radial uncertainty products calculated for three wave packets with the same $\sigma_n=2.5$, for $\bar{n}=80$, 320, and 1000, are equal to 0.642, 0.539, and 0.513, respectively.

The expectation value of the azimuthal angle in a circular-orbit state is $\langle\theta\rangle=\pi/2$. The expectation value of the square of the azimuthal angle is equal to

$$\langle\theta^2\rangle_n=\frac{\pi^2}{4}+2\sum_{k=n}^{\infty}\frac{1}{(2k+1)^2} \quad (5)$$

and the uncertainty in this angle is equal to the square root of the sum in Eq. (5). This sum is estimated to be within the limits

$$\frac{1}{4(n+1)}\left[1+\frac{3}{2(n+2)}\right]<\sum_{k=n}^{\infty}\frac{1}{(2k+1)^2}<\frac{1}{4n}\left[1+\frac{3}{2(n+1)}\right].$$

The expectation value of the azimuthal momentum in any eigenstate is equal to zero, whereas the expectation value of its square can be calculated as

$$\langle L_\theta^2\rangle_n=\langle L^2\rangle_n+\langle L_z^2\rangle_n\left\langle\frac{1}{\sin^2\theta}\right\rangle_n=\frac{n-1}{2}$$

since $[L_z,\theta]=0$. The uncertainty product θ is then found to be

$$(\Delta\theta\Delta L_\theta)_n=\frac{1}{2}\left[1+\frac{1}{4n}\right]+O\left[\frac{1}{n^2}\right]. \quad (6)$$

The uncertainty product of the circular-orbit wave packet in the azimuthal degree of freedom is calculated using the same procedure as in the case of radial quantities, and is found to have the same value as the uncertainty product for a single circular-orbit state in Eq. (6) with n replaced by $\bar{n}$. For the same three initial wave packets as in the radial case, $\Delta\theta\Delta L_\theta$ is equal to 0.5016, 0.5004, and 0.5001, respectively.

In an aligned eigenstate, the probability of finding the electron at a point whose polar angle lies between ϕ and $\phi+d\phi$ is uniformly distributed around the circle of radius n^2, with an expectation value equal to π and a standard deviation equal to $\pi/\sqrt{3}$. A wave packet that is localized in the polar angle is formed by superimposing aligned wave functions. Localization in the polar angle is more complicated to calculate than in the other two degrees of freedom, because the operator ϕ is a conjugate

operator to L_z. Therefore, the uncertainty in ϕ was calculated numerically. The uncertainty in L_z is equal to σ_n. The uncertainty product in the polar degree of freedom for wave packets of width $\sigma_n=2.5$ and centered at $\bar{n}=80$ and 320 is equal to 0.635 and 0.5125, respectively.

In this section we calculated uncertainty products for Brown's quasiclassical state in all three degrees of freedom. We found that this state is almost a minimum-uncertainty wave packet. The excess uncertainty is a decreasing function of $\bar{n}$ and tends toward zero in the limit of large quantum numbers.

IV. DYNAMICS OF THE QUASICLASSICAL STATE OF THE HYDROGEN ATOM

The dynamics of a circular-orbit wave packet possesses both classical and quantum-mechanical features, and they are very intricately mixed. Initially, the well-localized wave packet travels around the nucleus in a Kepler circle and spreads along the orbit over a time of several classical periods. A circular-orbit wave packet with $\bar{n}=320$ and $\sigma_n=2.5$ is shown in Figs. 1(a)–1(e), at times separated by $T_{\text{Kepler}}/4$, where $T_{\text{Kepler}}=2\pi\bar{n}^3$ is the classical Kepler period of the corresponding classical particle.

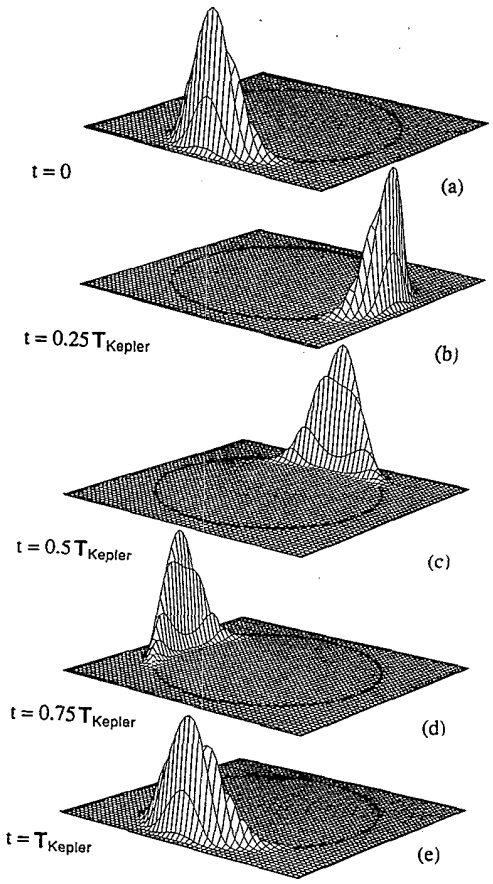

FIG. 1. (a)–(e) The initial stage of the evolution of the circular-orbit wave packet ($\bar{n}=320$, $\sigma_n=2.5$) at times 0, $\frac{1}{4}$, $\frac{1}{2}$, $\frac{3}{4}$, and 1 (in units of T_{Kepler}).

An electron wave packet can be thought of as an interference pattern of the weighted constituent eigenfunctions. Since each of these eigenfunctions evolves at a different frequency, the interference pattern will vary over time. Sometimes, the probability is distributed almost uniformly around the orbit, but at other times the interference pattern appears regular and consists of a number of almost identical wave packets distributed at equal intervals along the orbit. Parker and Stroud[21] pointed out quantum beats at frequencies equal to multiples of the classical orbital frequency in the fluorescence signal of the radial wave packet. These quantum beats were linked to multipacket formations and were called fractional revivals by Averbukh and Perelman.[22]

Spreading and revivals of the wave packet are a consequence of nonlinearity of the Hamiltonian of the hydrogen atom. Because of the nonlinearity, the energy levels are not equidistant and the wave packet spreads. The Taylor-series expansion of the time-dependent phase in Eq. (2) is

$$\frac{t}{2n^2}=\frac{t}{2\bar{n}^2}\left[1-2\frac{\Delta n}{\bar{n}}+3\left[\frac{\Delta n}{\bar{n}}\right]^2-4\left[\frac{\Delta n}{\bar{n}}\right]^3+5\left[\frac{\Delta n}{\bar{n}}\right]^4-\cdots\right], \tag{7}$$

where $\Delta n=n-\bar{n}$. In the early stages of the evolution of the wave packet, only the linear term in expression (7) is important and the state vector is

$$|\Psi_{\text{class}}(t)\rangle=\sum_{n=1}^{\infty} w_n|\Psi_{n,n-1,n-1}(t)\rangle \times\exp\left[-\frac{2\pi i n t}{T_{\text{Kepler}}}\right], \tag{8}$$

where w_n is a Gaussian weighting factor. Equation (8) describes a wave packet that moves in a classical orbit and, as a result of the linearization, preserves the initial form.

The contribution of the second-order term in Eq. (7) becomes significant after a time of the order of $2T_{\text{Kepler}}\bar{n}/3(\Delta n_{\max})^2$, where $\Delta n_{\max}=n_{\max}-\bar{n}$. The principal quantum number $n_{\max}$ refers to the level farthest from the $\bar{n}$th level that is still significantly populated. Spreading and revivals of the wave packet can be explained as a result of the second-order term. The initial spreading of the wave packet along the orbit is approximately described by the variance[8] $\Delta\phi^2$ at time t,

$$\Delta\phi^2=\sigma_n^2+\frac{2\pi}{\sigma_n^2 2T_{\text{rev}}}, \tag{9}$$

where $T_{\text{rev}}=(\bar{n}/3)T_{\text{Kepler}}$ is the revival time defined by Parker and Stroud.[21] They predicted that an almost complete revival of the radial wave packet would occur after time T_{rev}. This prediction was recently confirmed in the experiment by Yeazell and Stroud.[23] Equation (9) is obtained when the sum in Eq. (1) is replaced by an in-

tegral and only the dependence on the polar angle is taken into account. The resulting integral is a Fourier transform over n of a Gaussian function with a complex variance, which, in turn, is also a Gaussian function with the variance given by Eq. (9).

The time in which the initial packet spreads completely is calculated by equating the right-hand side of Eq. (9) with $\pi^2/3$, the value of the variance for a random variable uniformly distributed around the circle. We found that $T_{\text{spread}} = T_{\text{rev}}/8.713 = 12.2 T_{\text{Kepler}}$ for the wave packet with $\sigma_n = 2.5$ and $\bar{n} = 320$. Figures 2(a)–2(e) show spreading of this wave packet after 2.5, 5, 7.5, 10, and 12.5 classical periods. The spreading is smooth along the orbit until the tail of the wave packet meets with its head as shown in Figs. 2(a)–2(c); at this point a new interference pattern begins to form and small wave packets emerge, as in Figs. 2(d) and 2(e), in anticipation of the first fractional revival.

Revivals occur because the nonlinear phases of the individual constituent wave functions experience fractional periodicity[22] at moments that are embedded in time like rational numbers in real numbers. In other words, fractional revivals occur, theoretically, at any time $t = (k_1/k_2) T_{\text{rev}}$, where k_1 and k_2 are two mutually prime numbers. Very high fractional revivals are obscured because of the finiteness of the width of the initial wave packet.

During a fractional revival the wave packet is separated into K almost identical wave packets, and its state vector is[22]

$$|\Psi(t)\rangle = \sum_{k=0}^{K-1} a_k \left| \Psi_{\text{class}} \left[t + \frac{k T_{\text{Kepler}}}{K} \right] \right\rangle , \tag{10}$$

where a_k is a phase factor and $|\Psi_{\text{class}}(t)\rangle$ is defined in Eq. (8). The first distinct fractional revival will occur after time $T_{\text{rev}}/K_{\max}$, where $K_{\max}$ is the maximum number of

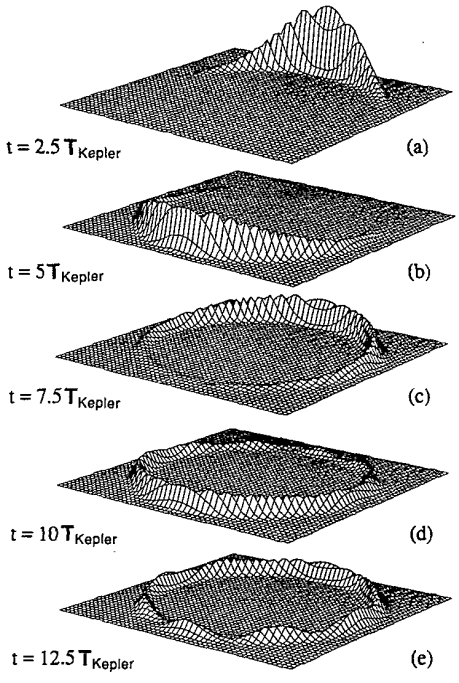

FIG. 2. (a)–(e) Spreading of the circular-orbit wave packet ($\bar{n} = 320$, $\sigma_n = 2.5$). The wave packet is depicted at times 2.5, 5, 7.5, 10, and 12.5 (in units of T_{Kepler}).

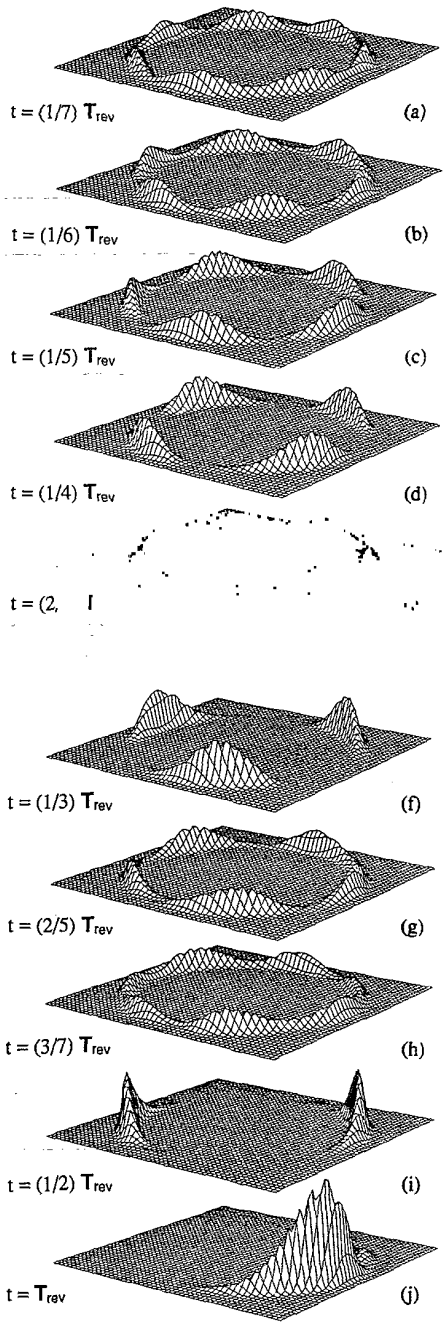

FIG. 3. (a)–(j) Fractional revivals of the circular-orbit wave packet ($\bar{n} = 320$, $\sigma_n = 2.5$) at times $\frac{1}{7}$, $\frac{1}{6}$, $\frac{1}{5}$, $\frac{1}{4}$, $\frac{2}{7}$, $\frac{1}{3}$, $\frac{3}{7}$, $\frac{2}{5}$, $\frac{1}{2}$, and 1 (in units of T_{rev}).

distinct wave packets that can be observed in a fractional revival. This number is a function of the initial width of the wave packet and can be easily calculated from the equation

$$\frac{T_{\text{rev}}}{K_{\max}} = T_{\text{spread}} + \frac{T_{\text{spread}}}{K_{\max}} .$$

For the same initial configuration of the wave packet as above, $K_{\max}$ is found to be between 7 and 8. All distinct fractional revivals of this wave packet until time $T_{\text{rev}}/2$ ($\frac{1}{7}$, $\frac{1}{6}$, $\frac{1}{5}$, $\frac{1}{4}$, $\frac{2}{7}$, $\frac{1}{3}$, $\frac{3}{7}$, $\frac{2}{5}$, and $\frac{1}{2}$ in units of T_{rev}) are shown in Figs. 3(a)–3(i), as well as the first "complete" revival after time T_{rev} in Fig. 3(j).

The second-order nonlinearity also causes a shift in the position of the revived wave packet, with respect to the prediction of the classical equations of motion. In all odd revivals the phase of the wave packet differs by π from the linear phase. As an example, compare the position of the wave packet in its first revival in Fig 3(j) with the position predicted by the classical equations of motion, which is $4\pi/3$ from the initial position.

After a time of the order of $T_{\text{Kepler}}\bar{n}^2/2(\Delta n_{\max})^3$, the contribution of the third-order term becomes significant. The phase shift associated with this contribution has a destructive effect on the regularity of the interference pattern. For example, the small wave packet that precedes the main wave packet in the first revival in Fig. 3(j) is a manifestation of the third-order contribution. Similarly, fourth- and higher-order contributions to the phase become increasingly important at later times. The way to extend the time during which nonlinear effects are not important is to superimpose the constituent eigenfunctions with a Gaussian weighting function narrower than the one used in our examples.

V. CONCLUSIONS

We studied the dynamics of a circular-orbit wave packet and found that, despite its many classical features, its quantum nature is always present. The classical aspect of the dynamics is most pronounced at the time of revivals, when a single well-localized wave packet travels along a Kepler orbit. Spreading and fractional revivals of the wave packet are manifestations of the quantum nature of the system, in particular the discreteness of the energy levels. In order to illustrate this fact, one can form a classical ensemble whose probability distribution is equal to the square of the modulus of the packet wave function. The initially well-localized ensemble spreads along the orbit until the particles become uniformly distributed. Needless to say, the classical "wave packet" does not reassemble because its Poincaré recurrence time is extremely long.

From the simple example that we studied in this paper, we learned that the large-quantum-number limit of the hydrogen atom has all the properties of a good quasiclassical state over the period of time during which the nonlinearity of the Hamiltonian may be ignored. After this time, the quantum nature of the system plays a major role in its evolution.

The classical limit of quantum mechanics is a topic of increasing importance in physics. At the time when atoms can be made larger than living cells and single ions kept in isolation for many hours, the border line between the microscopic and macroscopic worlds is no longer defined in a simple fashion.

ACKNOWLEDGMENTS

This work was supported by the Joint Services Optics Program. Z. D. G. would like to thank Christopher Gerry, Jonathan Parker, and John Yeazell for useful discussions and for bringing some of the references to her attention.

[1]N. Bohr, Z. Phys. **2**, 423 (1920).
[2]H. A. Kramers, K. Dan. Vidensk. Selsk. Skr. Naturvidensk. Math. Afd. **8**, III.3 (1919); L. Bloch, J. Phys. **3**, 110 (1922).
[3]J. G. Leopold and I. C. Percival, Phys. Rev. Lett. **41**, 944 (1978).
[4]E. J. Galvez, B. E. Sauer, L. Moorman, P. M. Koch, and D. Richards, Phys. Rev. Lett. **61**, 2011 (1988).
[5]V. P. Gutschick and M. M. Nieto, Phys. Rev. D **22**, 403 (1980); C. C. Gerry and J. Kiefer, Phys. Rev. A **37**, 665 (1988).
[6]E. Schrödinger, Naturwissenschaften **14**, 664 (1926).
[7]E. Schrödinger, in *Letters on Wave Mechanics,* edited by K. Prizibram (Philosophical Library, New York, 1967).
[8]L. S. Brown, Am. J. Phys. **41**, 525 (1973).
[9]A. O. Barut and L. Girardello, Commun. Math. Phys. **21**, 41 (1971).
[10]A. M. Perelomov, Commun. Math. Phys. **26**, 222 (1972).
[11]M. M. Nieto and L. M. Simmons, Jr., Phys. Rev. Lett. **41**, 207 (1978).
[12]J. Mostowski, Lett. Math. Phys. **2**, 1 (1977).
[13]D. S. MacAnnaly and A. J. Bracken J. Phys. A (to be published).
[14]C. C. Gerry, Phys. Rev. A **33**, 6 (1986).
[15]D. Bhaumik, B. Dutta-Roy, and G. Ghosh, J. Phys. A **19**, 1355 (1986).
[16]P. Kustaanheimo and E. Stiefel, J. Reive. Angew. Math. **218**, 204 (1965).
[17]S. Nandi and C. S. Shastry, J. Phys. A **22**, 1005 (1989).
[18]M. Nauenberg, Phys. Rev. A **40**, 1133 (1989).
[19]J. A. Yeazell and C. R. Stroud, Jr., Phys. Rev. Lett. **60**, 1494 (1988).
[20]H. A. Bethe and E. E. Salpeter, *Quantum Mechanics of One- and Two-Electron Atoms* (Plenum, New York, 1977).
[21]J. Parker and C. R. Stroud, Jr., Phys. Rev. Lett. **56**, 716 (1986).
[22]J. Sh. Averbukh and N. F. Perelman, Phys. Lett. **A139**, 449 (1989).
[23]J. A. Yeazell, M. Mallalieu, and C. R. Stroud, Jr., Phys. Rev. Lett. **64**, 2007 (1990).